Synthetic Landau Levels and Spinor Vortex Matter on a Haldane Spherical Surface with a Magnetic Monopole

Xiang-Fa Zhou,[1,2] Congjun Wu,[3] Guang-Can Guo,[1,2] Ruquan Wang,[4,5] Han Pu,[6,7,*] and Zheng-Wei Zhou[1,2,†]
[1]*Key Laboratory of Quantum Information, Chinese Academy of Sciences, University of Science and Technology of China, Hefei 230026, China*
[2]*Synergetic Innovation Center of Quantum Information and Quantum Physics, University of Science and Technology of China, Hefei 230026, China*
[3]*Department of Physics, University of California, San Diego, San Diego, California 92093, USA*
[4]*Institute of Physics, Chinese Academy of Sciences, Beijing 100080, People's Republic of China*
[5]*Collaborative Innovation Center of Quantum Matter, Beijing, China*
[6]*Department of Physics and Astronomy, and Rice Center for Quantum Materials, Rice University, Houston, Texas 77251, USA*
[7]*Center for Cold Atom Physics, Chinese Academy of Sciences, Wuhan 430071, People's Republic of China*

(Received 7 November 2017; published 29 March 2018)

We present a flexible scheme to realize exact flat Landau levels on curved spherical geometry in a system of spinful cold atoms. This is achieved by applying the Floquet engineering of a magnetic quadrupole field to create a synthetic monopole field in real space. The system can be exactly mapped to the electron-monopole system on a sphere, thus realizing Haldane's spherical geometry for fractional quantum Hall physics. This method works for either bosons or fermions. We investigate the ground-state vortex pattern for an s-wave interacting atomic condensate by mapping this system to the classical Thompson's problem. The distortion and stability of the vortex pattern are further studied in the presence of dipolar interaction. Our scheme is compatible with the current experimental setup, and may serve as a promising route of investigating quantum Hall physics and exotic spinor vortex matter on curved space.

DOI: 10.1103/PhysRevLett.120.130402

Introduction.—The realization of quantum Hall physics (QHP) in neutral atoms remains one of the long-standing goals in the cold atom community [1–9]. Theoretically, atomic systems not only provide an excellent platform to explore such novel physics for both bosons and fermions, the former is beyond the usual condensed matter systems, but also enable us to test various predictions with high precision due to its cleanness and high controllability. Experimentally, exact flat Landau levels can be obtained, in principle, by rotating the confining harmonic potential [10–13] with a frequency equal to that of the harmonic trap. However, in this limit, effective trapping potential vanishes, and the atomic cloud loses confinement. This makes it almost impossible to reach the exact quantum Hall regime using this setup [12]. Therefore, searching for new flexible methods of realizing QHP becomes important.

On the other hand, QHP becomes more clear in a modified geometry, as pointed out by Haldane in 1983 [14], who showed that a spherical surface trap with monopole [15–17] at the origin can be used as a prototype to understand such novel physics. The simplicity of this mode not only makes it an ideal numerical starting point to tackle this complex many-body system [18,19], but also reveals how interesting physics can be induced in curved spaces with the help of magnetic monopoles. Unfortunately, direct realization of this beautiful model seems impossible as no real magnetic monopole has been found.

In this paper, we show that, within current technique, exact Landau levels on Haldane's spherical geometry can indeed be implemented in a highly controllable manner. The key ingredient is the construction of synthetic monopole field in real space [20]. We prove that this is possible by using atoms with internal spin degrees of freedom [28–36] subjected to a Floquet engineered magnetic quadrupole field. By projecting the atom into the lowest-energy spin manifold using the technique developed by Ho and Huang in [37], we confirm that the single-particle physics is mapped to an electron-monopole system [14,15] on a sphere. This is exactly the Hamiltonian on a curved sphere with flat Landau levels, as originally envisioned by Haldane, which enables the exploration of QHP using neutral atoms with high tunability.

As a first step, we investigate the exotic ground-state vortex pattern in this curved geometry for Bose condensates. For s-wave interaction, we show that a stable vortex pattern can be well described by the standard Thompson's problem, which serves as a direct verification of charge-vortex duality in a two-dimensional system. For dipolar atoms, the anisotropy of dipole-dipole interaction breaks the rotational symmetry, which results in the accumulation of vortices around the poles and the equator, and can lead to an

instability. We note that the effect of the underlying geometry on various quantum orders has been widely considered [37–52], and only addressed recently for condensates on a cylindrical surface [37]. Our work thus provides a promising route of exploring various novel spinor vortex matter involved in a curved spherical geometry.

Realization of the synthetic monopole field.—Our scheme of realizing the synthetic monopole field for cold atoms can be outlined as follows. We start by considering an atom with hyperfine spin $\mathbf{F}$ subject to a magnetic field

$$\mathbf{B} = B_0\vec{z} + B_1[1 - 4\lambda\cos(\omega t)](x\vec{x} + y\vec{y} - 2z\vec{z}). \quad (1)$$

The magnetic field consists of a strong static bias field along the z axis with magnitude B_0, and a time-periodic quadruple field with driving frequency ω. We note that a static version of $\mathbf{B}$ has also been used by Ho and Huang [37] to induce artificial gauge fields on a cylinder. The interaction between the atomic magnetic dipole and the field leads to the Zeeman Hamiltonian $\tilde{H}_F = -\mu_B g_F \mathbf{F}\cdot\mathbf{B}$ with μ_B being the Bohr magneton and g_F the corresponding Landé g factor. For simplicity, here we neglect the quadratic Zeeman term proportional to $(\mathbf{B}\cdot\mathbf{F})^2 \simeq B_0^2 F_z^2$, which can be compensated by a proper choice of λ [see Supplemental Material (SM) [53] for details].

The effects induced by the strong bias field B_0 can be removed by transforming the whole system into the rotating frame defined by the unitary operator

$$U = \exp(-i\omega_L t F_z), \quad (2)$$

where $\omega_L \equiv \mu_B g_F B_0/\hbar$ is the Larmor frequency for the bias field. The Hamiltonian in the rotating frame is given by $H_F = U^\dagger \tilde{H}_F U - iU^\dagger\partial_t U$. Under the condition $\omega = \omega_L$; i.e., the driving frequency of the quadruple field matches with the Larmor frequency, and furthermore when ω is much larger than all other energy scales, the Hamiltonian in the rotating frame takes the following form [54], $H_F \simeq \mu_B g_F B_1[2\lambda(xF_x + yF_y) + 2zF_z]$, where the fast oscillating terms have been neglected. The above Hamiltonian can be recast into the form [53]

$$H_F = 2\mu_B g_F B_1 \lambda r(\mathbf{F}\cdot\vec{e}_r + \gamma\cos\theta F_z), \quad (3)$$

where $r = \sqrt{x^2+y^2+z^2}$ is the radial coordinate, $\vec{e}_r$ is the radial unit vector, and $\gamma \equiv 1/\lambda - 1$. In the following, we mainly focus on the situation $\lambda = 1$ or $\gamma = 0$, under which Hamiltonian (3) describes an atom with magnetic dipole moment moving in a radial magnetic field, whose strength increases linearly with r. If the atom is confined on a spherical shell surface (which is the case we focus on below), this radial magnetic field is equivalent to a monopole field.

Single-particle Hamiltonian.—Now we consider the full single-particle Hamiltonian, which includes H_F (with $\gamma = 0$) and an isotropic harmonic trapping potential $V = m\omega_T^2 r^2/2$ with m being the atomic mass, ω_T the harmonic trap frequency, and $l_T = \sqrt{\hbar/m\omega_T}$ the characteristic length. In the unit system defined by $\hbar = m = \omega_T = 1$, the single-particle Hamiltonian takes the form

$$H_0 = -\frac{\vec{\nabla}^2}{2} + \frac{1}{2}r^2 + \alpha' r\mathbf{F}\cdot\vec{e}_r, \quad (4)$$

where $\alpha' \equiv 2\mu_B g_F B_1(\hbar m\omega_T^3)^{-1}$ measures the strength of Zeeman coupling with the synthetic monopole field. Here and in the following, we assume $\alpha' > 0$ without loss of generality. Under this convention, the lowest spin manifold corresponds to the spin state that is polarized along the local monopole field and obeys $\mathbf{F}\cdot\vec{e}_r|F,-F\rangle_{\mathbf{r}} = -F|F,-F\rangle_{\mathbf{r}}$. In the F_z representation, we have $|F,-F\rangle_{\mathbf{r}} = \exp(-iF_z\varphi)\times\exp(-iF_y\theta)|F,-F\rangle_{\mathbf{z}}$, where θ and φ are the polar and the azimuthal angles, respectively.

Under the assumption that the atom adiabatically follows the local monopole field and thus stays in the lowest spin manifold [37,53], we can write the total wave function of the atom as $\psi(\vec{r}) = \phi(\vec{r})|F,-F\rangle_{\mathbf{n}}$, where $\phi(\vec{r})$ is the spatial wave function. After projecting out the spin component, we find that $\phi(\vec{r})$ is governed by the following effective Hamiltonian (see SM [53] for details),

$$H_{\text{eff}} = \frac{(-i\vec{\nabla} + \vec{A})^2}{2} + V(r), \quad (5)$$

where $\vec{A}(\vec{r}) = F(\cos\theta/r\sin\theta)\vec{e}_\varphi$ is the effective gauge potential, and $V(r) = r^2/2 - \alpha r + F/2r^2$ with $\alpha = \alpha' F$ being the effective trapping potential. When $\alpha \gg 1$, $V(r)$ has a minimum at $r = R \approx \alpha$, and the atom is tightly confined near this minimum with negligible radial excitation. Under this condition, the radial degrees of freedom are frozen and the spatial wave function is reduced to $\phi(\vec{r}) = h(r)f(\theta,\varphi)$, where $f(\theta,\varphi)$ is governed by the reduced Hamiltonian

$$H = \frac{1}{2R^2}\Lambda^2, \quad (6)$$

with $\mathbf{\Lambda} = \vec{r}\times[-i\vec{\nabla} + \vec{A}(\vec{r})]$.

Hamiltonian (6) describes a charged particle confined on a spherical surface with radius Rl_T subject to a magnetic monopole with charge proportional to F centered at the origin. The model was studied by Dirac, Wu-Yang, and many others to clarify the quantization of monopole charge [16,17], and later used by Haldane as an alternative spherical geometry to understand the fractional QHP (FQHP) [14]. The single-particle eigenstates are given by the monopole harmonics $\mathcal{Y}_{l,F}^m$ [53,55,56] with $l = F, F+1, \cdots$ and $m = -l, -l+1, \ldots, l$. The corresponding

energy eigenvalues are $E_k = [l(l+1) - F^2]/(2R^2)$ with $k = l - F$, which leads to a Landau-level-like structure.

The above construction of Haldane spherical surface provides a unique way to explore FQHP using neutral atoms. First, unconstrained expansion of the atomic cloud is avoided due to the finite size of the surface. The exact flatness of Landau levels enables that FQHP can be easily manifested with only a few particles by tuning the interaction effect via Feshbach resonance using magnetic field, or by changing the density of the cloud [10–12]. Second, the simplicity of the model makes it possible for the direct comparison between experimental and theoretical results [18,19], which provides an ideal test bed for various theoretical predictions about FQHP. Third, the high flexibility of the system also enables the investigation of novel quantum matter related to QHP and curved spherical geometry, as we show in the following.

Ground-state vortex structure for condensate with contact interaction.—We now consider the properties of a weakly interacting atomic condensate. The reduced condensate wave function $f(\hat{\Omega}) = f(\theta, \varphi)$, defined above Eq. (6), satisfies the following Gross-Pitaevskii (GP) equation:

$$i\partial_t f(\hat{\Omega}) = \left(\frac{\Lambda^2}{2} + g|f(\hat{\Omega})|^2 + g_d D(\hat{\Omega})\right) f(\hat{\Omega}), \quad (7)$$

where for simplicity, we have rescaled the radius of the sphere to be the units for length; the second term in the large parentheses describes the contact s-wave interaction characterized by the dimensionless interaction strength $g \simeq 2\sqrt{2\pi} N a/l_T$, with a being the s-wave scattering length and N the number of atoms; the third term describes the dipolar interaction characterized by strength g_d, and the form of $D(\hat{\Omega})$ depends on the orientation of the atomic dipole, whose explicit form is given in SM [53].

For nondipolar condensate with $g_d = 0$ and with weak contact interaction, since the single-particle eigenstates in the lowest Landau level (LLL) can be written as $\mathcal{Y}^m_{F,F} \sim u^{F-m} v^{F+m}$ with $u = \cos(\theta/2) e^{-i(\varphi/2)}$ and $v = \sin(\theta/2) e^{i(\varphi/2)}$, a general wave function within this subspace can be expressed as $f(\hat{\Omega}) = \sum_{m=0}^{2F} c_m u^{F-m} v^{F+m}$, which can then be factorized as $\Pi_{j=1}^{2F}(u v_j - u_j v)$ up to a normalization constant. This describes a lattice of $2F$ vortices, with (u_j, v_j) representing the coordinates of the vortices on the sphere. The interaction energy is written as $U_{\text{int}} \sim \int d\hat{\Omega} |f(\hat{\Omega})|^4$ with

$$|f(\hat{\Omega})|^2 = e^{-K}, \quad \text{and} \quad K \sim -2\sum_j \ln|u v_j - u_j v|, \quad (8)$$

where $|u v_j - u_j v|$ is the chord distance between two points on the unit sphere. The quantity K precisely describes the energy of an electron interacting with $2F$ other electrons located at (u_j, v_j). Therefore, minimization of U_{int} with respect to (u_j, v_j) can be mapped to the problem of finding the stable configuration of $2F$ electrons on a sphere. This is exactly the well-known Thomson's problem, as J. J. Thomson posed such a model to understand his plum pudding model of the atom in 1904 [59].

We have obtained the ground state by solving the GP equation (7) using the imaginary evolution method [53,57,58] without taking the LLL approximation. The ground-state vortex configuration for F up to 8 is shown in Fig. 1. For each F, the pattern consists of $2F$ vortices and is equivalent to (up to a global rotation) the standard solutions to Thomson's problem, which is a direct reflection of charge-vortex duality in two-dimensional systems. We note that the Thomson's lattice is stable for g up to 500 (the largest value we tested numerically), which is far beyond the usual LLL approximation as the dimensionless magnetic length $l_m = \sqrt{1/F}$ is much larger than the healing length $\xi = \sqrt{2\pi/g}$ [53]. The singularity of $\vec{A}$ at the two poles in our chosen gauge can be removed after projecting the wave function back to the usual Zeeman manifolds. For each Zeeman sublevel, there is a giant vortex with $\mp F + F_z$ units of circulation around the north and south poles, respectively, as shown in SM [53].

Stability and vortex structure in dipolar condensate.—We now include the dipolar interaction term in the Hamiltonian, which is very typical for condensates of atoms with large internal spin. For an atom with spin $\mathbf{F}$, it possesses a magnetic dipole moment $\vec{\mu} = \mu_B g_F \mathbf{F}$. Given two dipoles $\vec{\mu}_1$ and $\vec{\mu}_2$ located at $\vec{r}_1$ and $\vec{r}_2$, respectively, the dipolar interaction in the lab frame reads $U_d(\vec{r}_1, \vec{r}_2) = [\vec{\mu}_1 \cdot \vec{\mu}_2 - 3(\hat{r}_{12} \cdot \vec{\mu}_1)(\hat{r}_{12} \cdot \vec{\mu}_2)]/r_{12}^3$ with $r_{12} = |\vec{r}_1 - \vec{r}_2|$ and $\hat{r}_{12} = (\vec{r}_1 - \vec{r}_2)/r_{12}$. In the rotating frame defined by the unitary operator U in Eq. (2), it transforms as $U_d(\vec{r}_1, \vec{r}_2) \to U^\dagger U_d U$, and becomes time dependent. In this case, each local spin rotates around the z axis with the frequency ω_L, as shown in Fig. 2(a). After integrating out

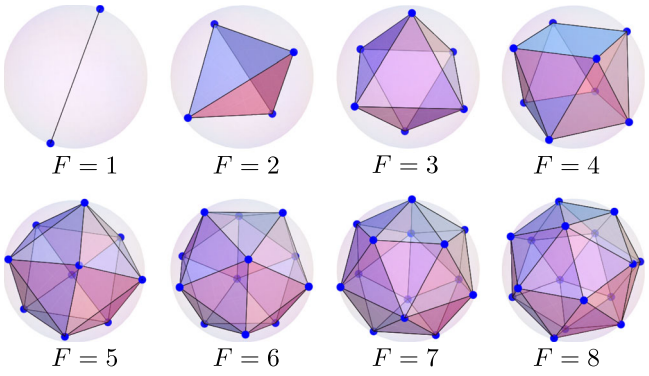

FIG. 1. Stable ground-state vortex configurations with isotropic s-wave interaction $g = 50$ for different F. Here the locations of the vortex cores are represented with blue dots on the spherical surface.

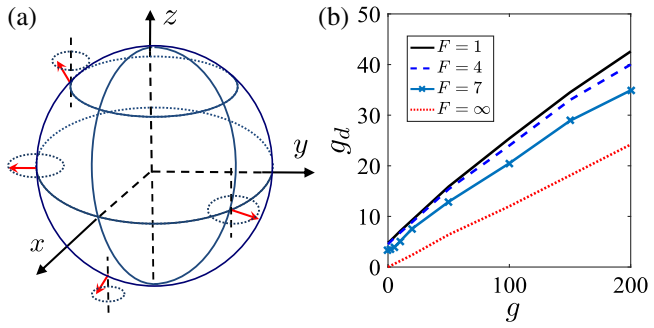

FIG. 2. Modulated dipolar orientation on the spherical surface and the critical $g_d^{(c)}$ along with repulsion g for different F. (a) In the interaction picture, each local dipole rotates around the z axis with frequency ω_L, which results in an average dipolar interaction described by Eq. (9). (b) shows the stability diagram in the $g_d - g$ plane. The condensates are unstable when $g_d > g_d^{(c)}$. The critical $g_d^{(c)}$ decreases along with F, and approaches the limit dotted line for $F \to \infty$.

the high-frequency parts, we arrive at an effective time-independent dipolar interaction potential as (see SM [53] for details)

$$U_d^{(e)}(\vec{r}_1, \vec{r}_2) = \frac{1}{r_{12}^3}\sqrt{\frac{6\pi}{5}} Y_2^0(\hat{\Omega}_{12}) \Sigma_2^0(\vec{\mu}_1, \vec{\mu}_2), \tag{9}$$

with $\hat{\Omega}_{12}$ being the orientation of $\vec{r}_{12}$ and $\Sigma_2^0(\vec{\mu}_1, \vec{\mu}_2) = \sqrt{2/3}(\vec{\mu}_1 \cdot \vec{\mu}_2 - 3\mu_{1,z}\mu_{2,z})$. Therefore, the interaction breaks the rotational symmetry, which modifies the distribution of the condensate and distorts the vortex pattern obtained in the previous section.

The anisotropicity of $U_d^{(e)}(\vec{r}_1, \vec{r}_2)$ can be illustrated from its local properties. For two neighboring sites represented as $\vec{r}' = \vec{r} + \delta(\cos\alpha \vec{e}_\theta + \sin\alpha \vec{e}_\phi)$ with δ being an infinitesimal arc length and α the azimuthal angle in the local tangent plane, the diploar interaction can be written as

$$U_d^{(e)}(\vec{r}, \vec{r}') \propto \frac{(3\cos^2\alpha \sin^2\theta - 1)(1 - 3\cos^2\theta)}{\delta^3}. \tag{10}$$

When $\vec{r} - \vec{r}'$ is parallel with the longitude with $\alpha = 0$, $U_d^{(e)}(\vec{r}, \vec{r}')$ becomes attractive for $\theta \in [\theta_2, \theta_1] \cup [\pi - \theta_1, \pi - \theta_2]$ with $\theta_1 = \cos^{-1}\sqrt{1/3}$ and $\theta_2 = \cos^{-1}\sqrt{2/3}$. However, when $\vec{r} - \vec{r}'$ coincides with the latitude, $U_d^{(e)}(\vec{r}, \vec{r}')$ is attractive only around the equator with $\theta \in [\theta_1, \pi - \theta_1]$. This azimuth-dependent attractive interaction can result in instability and collapses the condensates. The average local dipolar interaction can be estimated by integrating over the angle α and reads $\bar{U}_d^{(e)}(\vec{r}, \delta) \propto (1 - 3\cos^2\theta)^2/(2\delta^3)$, which is minimized at $\theta = \theta_1$ and reaches its local maxima when $\theta = 0$ (or π) and $\pi/2$.

Figure 2(b) shows the critical dipolar interaction strength $g_d^{(c)}$ as a function of contact interaction strength g for different spin F. The condensate is stable below the critical line, and unstable above it. The critical $g_d^{(c)}$ decreases as F increases. Physically, this can be understood by noticing that the degeneracy of single-particle ground state (i.e., the lowest Landau level) increases linearly with F. For larger F, the condensate has more degrees of freedom to adjust its wave function within the lowest Landau level to lower the interaction energy, while the kinetic energy almost remains unaffected. In the limiting case $F \to \infty$, the kinetic energy is complete quenched, and the stability of the condensate is solely determined by the relative strength of the contact repulsion and the dipolar interaction. This critical $g_d^{(c)}$ for $F = \infty$ is represented by the dotted line shown in Fig. 2. Our numerical results for finite F provide a direct verification towards this limit.

We note that for condensates with strong dipolar interaction near the critical $g_d^{(c)}$, the vortex configuration also deviates significantly from the standard Thomson's lattice, particularly for large F, as depicted in Fig. 3. Compared with s-wave contact interaction, these patterns are equivalent up to a global rotation around the z axis. Since $\bar{U}_d^{(e)}(\vec{r}, \delta)$ reaches its local maxima at $\theta = 0$ (π)and $\pi/2$, to minimize the interaction energy, vortices appear first near the two poles, and later spread around the equator with the increasing of F. For all F, the density peaks around the two

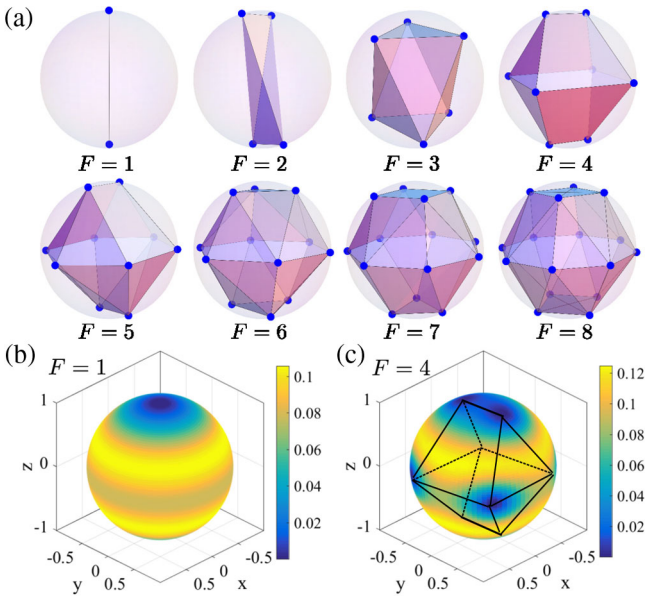

FIG. 3. Stable ground-state vortex configurations of dipolar Bose-Einstein condensate with $g = 50$ and different g_d. In (a), the data are obtained using $g_d = 10$ for $F = 1$–5 and $g_d = 8$ for $F = 6$–8, respectively. The vortex cores are represented with blue dots on the spherical surface. Since the dipole-dipole interaction breaks the rotation symmetry, the pattern is only equivalent up to a global rotation around the z axis for each F. (b) and (c) show the selected density portraits for $F = 1$ and $F = 4$, respectively. The vortices pattern is guided by lines and dot lines inside the sphere.

latitude lines with $\theta \sim \theta_1$ and $\pi - \theta_1$, respectively, as shown in Figs. 3(b) and 3(c). This can be understood from the average local dipolar interaction as $\bar{U}_d^{(e)}(\vec{r}, \delta)$ is minimized when $\theta = \theta_1$ and $\pi - \theta_1$.

Experimental feasibility.—For ^{168}Er [35] atoms with $F = 6$ in a bias magnetic field $\vec{B} = B_0\vec{z}$ with $B_0 = 0.30$ G, the linear Zeeman splitting is about $\omega = 2\pi \times 500$ kHz, which is much larger than the typical trapping frequency $\omega_T = 2\pi \times 2.5$ kHz. The radial length scale of the condensates is estimated as $l_T \simeq 0.246$ μm. To obtain an effective spherical-shell trap, we need $\alpha \simeq 0.48 B_1[\mathrm{cm\,G^{-1}}] \gg 1$. For the current experimental setup, it is not difficult to achieve a magnetic field gradient of $B_1 \simeq 20$ cm G^{-1}. This leads to $\alpha \sim R \sim 10 \gg 1$. Using these settings, the splitting of the first two Landau levels is $\Delta_L = (F+1)\omega_T/R^2 \sim 2\pi \times 175$ Hz, which is much smaller than the excitation energy ω_T along the radial direction. This ensures that condensates are only confined near the surface of the sphere. We note that for ^{87}Rb atoms with $F = 1$ [60–62], B_1 needs to be as high as 10^2–10^3 cm G^{-1}, which is still a challenge to the current experimental setup. Therefore, atomic species with large internal spin are always helpful for the construction of such a surface trap. The contact interaction can be estimated by $g \simeq 0.236N$. The relevant dimensionless healing length reads $\xi \simeq 5.16/\sqrt{N}$, which can then be tuned over wide parameter regimes by changing N compared with the magnetic length l_m.

Conclusion.—By constructing an effective hedgehoglike gradient magnetic field with spinful atoms, we have proposed a flexible way to implement an effective electron-monopole system confined on a spherical surface. We show how various vortex patterns can be obtained in the presence of interparticle interactions. The scheme proposed here provides a promising route to investigate the FQHP of bosons or fermions in curved space. Finally, the synthetic hedgehoglike gradient magnetic field for spinful atoms also provides new possibilities of searching for exotic spinor quantum matters related to magnetic monopoles [21–27,31].

This work was funded by National Natural Science Foundation of China (Grants No. 11474266, No. 11574294, and No. 11774332), the major research plan of the NSFC (Grant No. 91536219), the National Plan on Key Basic Research and Development (Grant No. 2016YFA0301700), and the "Strategic Priority Research Program (B)" of the Chinese Academy of Sciences (Grant No. XDB01030200). C. W. is supported by the Air Force Office of Scientific Research under Grant No. FA9550-14-1-0168. H. P. is supported by the U.S. NSF (Grant No. PHY-1505590) and the Welch Foundation (Grant No. C-1669). R. W. is supported by the National Basic Research Program of China (Grant No. 2013CB922002), and NSFC (Grant No. 11474347).

*hpu@rice.edu
†zwzhou@ustc.edu.cn

[1] L. Pitaevskii and S. Stringari, *Bose-Einstein Condensation and Superfluidity*, Vol. 164 (Oxford University Press, Oxford, 2016).
[2] M. Lewenstein, A. Sanpera, and V. Ahufinger, *Ultracold Atoms in Optical Lattices: Simulating Quantum Many-Body Systems* (Oxford University Press, Oxford, 2012).
[3] J. Dalibard, F. Gerbier, G. Juzeliūnas, and P. Öhberg, Rev. Mod. Phys. **83**, 1523 (2011).
[4] D. S. Jin and J. Ye, Chem. Rev. **112**, 4801 (2012).
[5] V. Galitski and I. B. Spielman, Nature (London) **494**, 49 (2013).
[6] X. Zhou, Y. Li, Z. Cai, and C. Wu, J. Phys. B **46**, 134001 (2013).
[7] H. Zhai, Int. J. Mod. Phys. B **26**, 1230001 (2012).
[8] D. Jaksch and P. Zoller, New J. Phys. **5**, 56 (2003).
[9] K. Osterloh, M. Baig, L. Santos, P. Zoller, and M. Lewenstein, Phys. Rev. Lett. **95**, 010403 (2005).
[10] S. Viefers, J. Phys. Condens. Matter **20**, 123202 (2008).
[11] A. L. Fetter, Rev. Mod. Phys. **81**, 647 (2009).
[12] N. R. Cooper, Adv. Phys. **57**, 539 (2008).
[13] S. Rachel, I. Göthel, D. P. Arovas, and M. Vojta, Phys. Rev. Lett. **117**, 266801 (2016).
[14] F. D. M. Haldane, Phys. Rev. Lett. **51**, 605 (1983).
[15] Y. M. Shnir, *Magnetic Monopoles* (Springer Science & Business Media, New York, 2006).
[16] P. A. Dirac, in *Proceedings of the Royal Society of London A: Mathematical, Physical, and Engineering Sciences* (The Royal Society, London, 1931), Vol. 133, pp. 60–72.
[17] T. T. Wu and C. N. Yang, Nucl. Phys. **B107**, 365 (1976).
[18] G. Fano, F. Ortolani, and E. Colombo, Phys. Rev. B **34**, 2670 (1986).
[19] F. D. M. Haldane and E. H. Rezayi, Phys. Rev. Lett. **54**, 237 (1985).
[20] We note that the current synthetic magnetic monopoles found in a spinor condensate are defined by the order parameters of the system [21–27], which cannot be used to induce an effective magnetic force on neutral atoms, as required by QHP.
[21] J. Ruostekoski and J. R. Anglin, Phys. Rev. Lett. **91**, 190402 (2003).
[22] V. Pietilä and M. Möttönen, Phys. Rev. Lett. **103**, 030401 (2009).
[23] M. W. Ray, E. Ruokokoski, S. Kandel, M. Möttönen, and D. Hall, Nature (London) **505**, 657 (2014).
[24] M. Ray, E. Ruokokoski, K. Tiurev, M. Möttönen, and D. Hall, Science **348**, 544 (2015).
[25] T. Ollikainen, K. Tiurev, A. Blinova, W. Lee, D. S. Hall, and M. Möttönen, Phys. Rev. X **7**, 021023 (2017).
[26] S. Sugawa, F. Salces-Carcoba, A. R. Perry, Y. Yue, and I. B. Spielman, arXiv:1610.06228.
[27] T.-L. Ho and C. Li, arXiv:1704.03833.
[28] C. Wu, Nat. Phys. **8**, 784 (2012).
[29] T.-L. Ho and S. Yip, Phys. Rev. Lett. **82**, 247 (1999).
[30] W. Yang, Y. Li, and C. Wu, Phys. Rev. Lett. **117**, 075301 (2016).
[31] Y. Kawaguchi, M. Nitta, and M. Ueda, Phys. Rev. Lett. **100**, 180403 (2008).

[32] T. Lahaye, C. Menotti, L. Santos, M. Lewenstein, and T. Pfau, Rep. Prog. Phys. **72**, 126401 (2009).
[33] Y. Kawaguchi and M. Ueda, Phys. Rep. **520**, 253 (2012).
[34] A. Griesmaier, J. Werner, S. Hensler, J. Stuhler, and T. Pfau, Phys. Rev. Lett. **94**, 160401 (2005).
[35] K. Aikawa, A. Frisch, M. Mark, S. Baier, A. Rietzler, R. Grimm, and F. Ferlaino, Phys. Rev. Lett. **108**, 210401 (2012).
[36] M. Lu, N. Q. Burdick, S. H. Youn, and B. L. Lev, Phys. Rev. Lett. **107**, 190401 (2011).
[37] T.-L. Ho and B. Huang, Phys. Rev. Lett. **115**, 155304 (2015).
[38] J. Batle, A. Bagdasaryan, M. Abdel-Aty, and S. Abdalla, Physica (Amsterdam) **451A**, 237 (2016).
[39] V. M. Fomin, R. O. Rezaev, and O. G. Schmidt, Nano Lett. **12**, 1282 (2012).
[40] J. Moody, A. Shapere, and F. Wilczek, Phys. Rev. Lett. **56**, 893 (1986).
[41] B. Zygelman, Phys. Rev. Lett. **64**, 256 (1990).
[42] B. Zygelman, J. Phys. B **46**, 134011 (2013).
[43] J. Yeo and M. A. Moore, Phys. Rev. B **57**, 10785 (1998).
[44] O. V. Pylypovskyi, V. P. Kravchuk, D. D. Sheka, D. Makarov, O. G. Schmidt, and Y. Gaididei, Phys. Rev. Lett. **114**, 197204 (2015).
[45] V. Parente, P. Lucignano, P. Vitale, A. Tagliacozzo, and F. Guinea, Phys. Rev. B **83**, 075424 (2011).
[46] S. K. Adhikari, Phys. Rev. A **85**, 053631 (2012).
[47] Y. Li and F. Haldane, arXiv:1510.01730.
[48] K.-I. Imura, Y. Yoshimura, Y. Takane, and T. Fukui, Phys. Rev. B **86**, 235119 (2012).
[49] Y. E. Kraus, A. Auerbach, H. A. Fertig, and S. H. Simon, Phys. Rev. Lett. **101**, 267002 (2008).
[50] S. Moroz, C. Hoyos, and L. Radzihovsky, Phys. Rev. B **93**, 024521 (2016).
[51] Z.-Y. Shi and H. Zhai, J. Phys. B **50**, 184006 (2017).
[52] J. Zhang and T.-L. Ho, arXiv:1707.09460.
[53] See Supplemental Material at http://link.aps.org/supplemental/10.1103/PhysRevLett.120.130402 for explicit derivation of the reduced Hamiltonian of the system, the ladder operators for monopole harmonics, and the calculation details about dipolar condensates, which includes Refs. [17,26,30,54–58].
[54] T. Isoshima, M. Nakahara, T. Ohmi, and K. Machida, Phys. Rev. A **61**, 063610 (2000).
[55] M. Greiter, Phys. Rev. B **83**, 115129 (2011).
[56] H. Fakhri, A. Dehghani, and A. Jafari, J. Math. Phys. (N.Y.) **48**, 023510 (2007).
[57] D. M. Healy, D. N. Rockmore, P. J. Kostelec, and S. Moore, J. Fourier Anal. Appl. **9**, 341 (2003).
[58] The fast spherical Fourier transformation is based on SpharmonicKit, a freely available collection of C programs for doing Legendre and scalar spherical transforms developed at Dartmouth College by S. Moore,D. Healy, D. Rockmore, and P. Kostelec; it is available at http://www.cs.dartmouth.edu/ geelong/sphere/.
[59] J. J. Thomson, Lond. Edinb. Dubl. Phil. Mag. **7**, 237 (1904).
[60] Z.-F. Xu, L. You, and M. Ueda, Phys. Rev. A **87**, 063634 (2013).
[61] B. M. Anderson, I. B. Spielman, and G. Juzeliūnas, Phys. Rev. Lett. **111**, 125301 (2013).
[62] X. Luo, L. Wu, J. Chen, Q. Guan, K. Gao, Z. Xu, L. You, and R. Wang, Sci. Rep. **6**, 18983 (2016).